Advances in Engineering Research, volume 208
Proceedings of the International Conference on Innovation in Science and Technology (ICIST 2020)

3D CFD Simulation Analysis of Drying Cabinet at Transient Condition

Arrad Ghani Safitra*, Lohdy Diana, Julfan Hafiz Farezza
Mechanic and Energy Department
Politeknik Elektronika Negeri Surabaya
Surabaya, Indonesia
*arradgs@pens.ac.id, lohdydiana@pens.ac.id, julfanhafiz@pg.student.pens.ac.id

***Abstract*—The drying cabinet had functioned as a storage hot air from the solar collector. There were some trays inside the drying cabinet. This paper had many purposes to predict air vector velocity and air temperature distribution inside the drying cabinet. It was done by simulation. It used computational fluid dynamics method with some setting such as the SIMPLE algorithm, k-epsilon realizable as a viscous turbulent model. The air inlet temperature was 323 K with a velocity of 0.1 m/s and 303 K for ambient temperature. It was simulated in a transient condition with time step 0.01 seconds. The velocity vector and temperature distribution were plotted at 4 seconds, 8 seconds, 16 seconds, and 32 seconds. The result showed tray in the bottom corner was the optimum tray. It was because of the position near to the inlet section or hot source with a maximum air temperature 322.6 K. It was also proved by air velocity streamlines that form big vorticities in the tray surface. At 32 seconds, air temperature distribution was already mixed and at the time the velocity vector reattachment formed. Its signed air temperature could be uniform if the number of iterations was increased.**

Keywords—simulation, drying cabinet, tray, velocity, temperature

I. INTRODUCTION

One of the renewable energies is solar. It could heat air for drying food, meat, fruit, and vegetables [1,2]. It was called a solar air heater. In a solar air heater, a drying cabinet was needed [3]. It had a function to collect hot air from the solar collector. The hot air would heat food or vegetables until it becomes dry. Food or vegetables were usually arranged on some trays inside the drying cabinet.

The experimental study of drying cabinet measured air temperature with some thermocouple were put in different position inside the drying cabinet [4]. Another experiment, a compact solar cabinet was tested to dry a lump of meat. The design of the cabinet dryer had a function to dry a lump of meat with solar energy. It had five trays. The result had revealed that this compact solar cabinet dryer had the same condition with an open sun drying and had a higher weight loss of the meat than an open sun drying [5]. The analysis was to evaluate solar cabinet drying performance equipped installed with an evacuated tube solar collector and thermal storage system with Phage Change Material (PCM) and modeled to CFD. The result of the analysis showed that the dryer with PCM could increase input thermal energy 1.72% and 5.12% at an airflow rate of 0.025 and 0.05 kg/s but decreased at over from 0.05kg/s. there had no adverse on a quality product in the use of PCM [6].

The research about the drying cabinet was not only experimentally but also done by simulation. Investigate product weight loss and display shelf life, using 2D Computational fluid dynamic to observe the effect of environmental boundary condition on drying rate and display shelf life. The higher the boundary layer value, the better the food quality, decrease the drying rate of the food product, and increase the display shelf-life [7]. A solar agricultural dryer with back-up biomass burner and thermal storage was simulated, numerical simulation was used for solar collector and drying chamber and used CFD to simulate the biomass burner. The results say that the temperature on the top tray is significantly higher [8]. Improved the biomass energy with recirculation of unidirectional airflow inside the drying cabinet. Numerical simulation based on solving Navier-Stokes was used to predict airflow. The result, the time to reduce the Khaitan moisture content was reduced, hence, better energy efficiency [9]. Mathematical modeling through CFD used to assess the drying chamber of a heat pump dryer from a drying air velocity and temperature profiles. The profile results showed that it was still needed to redesign the chamber. dryer products could only be achieved by trays 2, 3, and 4 that could [10]. The simulation drying chamber in three dimensions was done by transient condition until 44.59 seconds. It used k-epsilon as a turbulent viscous model [11].

This paper did a simulation of the drying cabinet in three dimensions it used computational fluid dynamics. Several previous types of research had been explained were used as references for this study. In this study, the geometry of the drying cabinet used five trays. There are many rectangle holes on trays. This simulation was a transient condition with time step 0.01 seconds and 32000 number of iterations. It meant from 0.01 s until 32 seconds. This paper had many purposes to predict some phenomena such as air vector velocity, air

temperature distribution, air velocity streamlines, change of air velocity, temperature, and pressure inside the drying cabinet. The data were plotted at 4 seconds, 8 seconds, 16 seconds, and 32 seconds. Based on simulation results optimum tray position could be determined.

II. Theorical Equation

A. Continuity Equation

This simulation used the continuity equation. It was represented the conservation of mass [9].

$$\frac{\partial \rho}{\partial t}\nabla.(\rho\vec{u}) = 0 \quad (1)$$

Where $\vec{u}$ is the fluid velocity and ρ is the density of air.

B. Momentum Equation

This simulation used the Navier Stokes equation momentum equation. It was used because there was air velocity [9].

$$\frac{\partial}{\partial t}(\rho\vec{u}) + (\rho\vec{u}\vec{u}) = -\nabla P + \nabla\bar{\bar{\tau}} + \rho\vec{g} + S_m \quad (2)$$

C. Energy Equation

This simulation needed hot air to input inside the drying cabinet. It means the energy equation must be activated [9].

$$\frac{\partial}{\partial t}(\rho E) + \nabla\cdot\left(\vec{u}(\rho E + P)\right) = P\nabla\cdot(-\vec{q} + \bar{\bar{\tau}}\cdot\vec{u}) + S_h \quad (3)$$

III. Methods

There were several steps in this simulation. The first step created drying cabinet geometry and mesh. Then, the parameter set was input after calculation, the result can be known. This section will explain the simulation method.

A. Drying Cabinet Model and Meshing

This simulation of the drying cabinet in three dimensions.

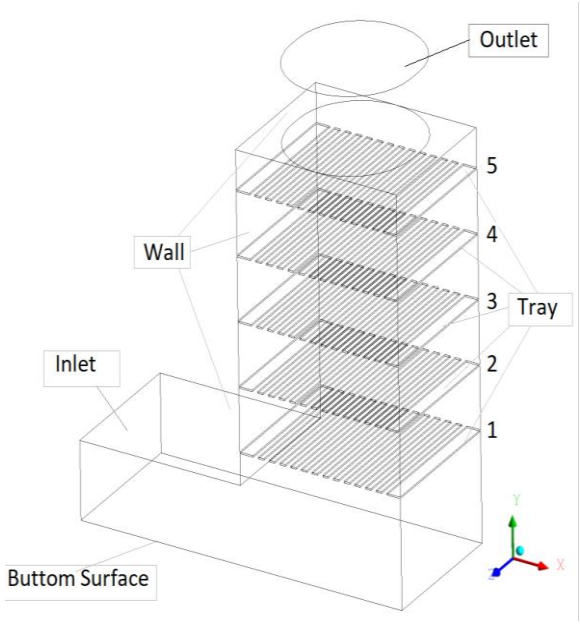

Fig. 1. Drying cabinet model.

The drying cabinet had 1.55 m in high, 1.2m in length, and 0.25 m in width. It can be seen in Figure 1. There were five trays inside the drying cabinet. The tray gap was 0.2 m. There are 13 rectangular holes in the tray surface. The hole width dimension was 20 mm.

Figure 2 shows meshing for the drying cabinet. The meshing type was tetrahedral. It had 14814 nodes and 71232 cells. The skewness was 0.01, it was under 0.9. It meant the quality of the mesh was good to produce an accurate simulation result.

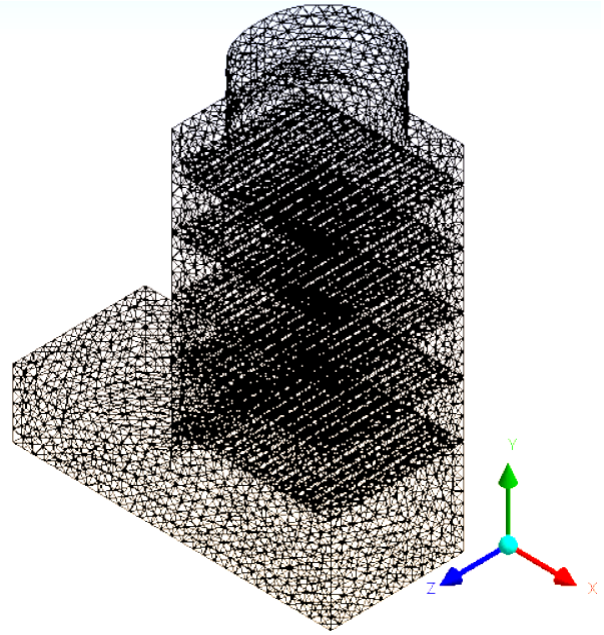

Fig. 2. Meshing.

B. Boundary Condition

The boundary condition for the inlet section in the drying cabinet was velocity inlet 0.1 m/s with air temperature 323 K. The drying cabinet walls boundary condition were wall with a constant temperature. It had a temperature the same with ambient temperature 303 K. The wall made from acrylic with some properties can be seen in Table 1. The outlet section was a pressure outlet, in this section the ventilator turbine was installed. The boundary condition of the surface bottom was a wall with no heat flux and no temperature constant. it's Because the surface bottom was insulated.

TABLE I. MATERIAL PROPERTIES

Acrylic Properties		
Properties	***Value***	***Unit***
Density	1.18	g/cm^{-3}
Thermal concudtivity	0.031	W/m.K
Heat capacitance	1465	J/kg.K

C. Parametter Setting in Transient Condition

This simulation used SIMPLE as the algorithm, k-epsilon realizable as a viscous turbulent model, second order for discretization for momentum, and residual monitoring used 10-4 for continuity and velocity in x, y, z direction, 10-6 for energy.

This simulation used the transient method. The time step is 0.01 seconds with the number of iterations 3200. It means running start from 0.01 seconds until 32 seconds. But this paper only presented simulation results at 4 seconds, 8 seconds, 16 seconds, and 32 seconds.

IV. RESULTS AND DISCUSSION

This section will discuss simulation results such as velocity vector inside the drying cabinet, air temperature distribution in the middle plane of the drying cabinet, and air temperature in each tray inside the drying chamber.

A. Verification

This study used air temperature in the outlet section as verification parameter. It would be compared with the experimental result. The air temperatures in the outlet section were 317 K for the experimental and 318.47 K for this simulation at 32 seconds. The error was 0.46 percent. It meant this simulation relative accurate.

B. Velocity Vector Inside Drying Cabinet

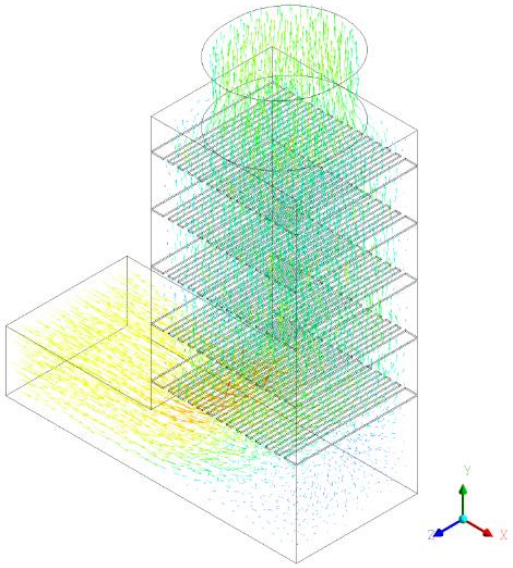

Fig. 3. Air velocity vector in isometric view.

The air velocity was drawn by vector when t = 32 seconds. It can be seen in Figure 3. It shows in the isometric view. Based on the figure, the air velocity in the inlet section and the outlet section was high. The air velocity from inlet section from x = 0 m to x = 600 m was uniform 0.01 m/s. It is signed by the same yellow colour. In outlet position y = 1.33 m to y = 1.55 m, the air velocity became high again different from the middle section. It because the ventilator turbine was installed in the outlet section. In position x = 0.6 m to x = 1.2 m and y = 0 m to y = 1.33 m, the air velocity was rather low.

It because of gravity acceleration and there are several trays inside the cabinet. Trays became as disturbance for air to go up. It was signed by a green colour vector. The airflow near the wall had a blue colour vector. It means low air velocity. It because the wall had a temperature the same with ambient temperature. The ambient temperature caused the cooling process. It would cool hot air.

The air velocity vectors were plotted in the middle plane for time 4 seconds until 32 seconds. The result can be seen in Figure 4. It had a purpose to know the different airflow patterns from time to time although the air velocity was constant 0.1 m/s. Based on Figure 5, when 4 seconds the airflow was a smooth pattern. The air entered the cabinet smoothly. The same pattern happened until 8 seconds. It meant air though from the inlet section to the outlet section directly.

Figure 5 shows when time 16 seconds, there was small reattachment in the bottom corner of the cabinet. It meant there was a mixing process inside the cabinet. The reattachment became big when 32 seconds. It caused air current could be mix with new air.

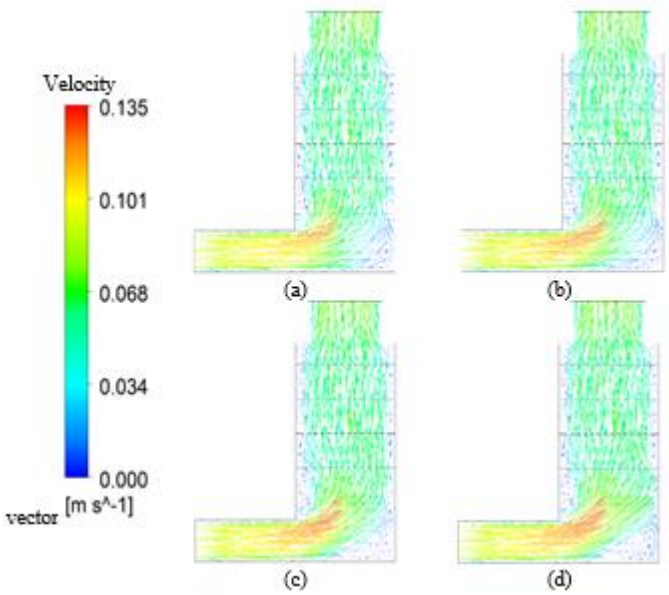

Fig. 4. Air velocity vector in middle plane (a) 4s, (b) 8s, (c) 16s, (d) 32s.

C. Air Temperature Distribution in Middle Plane

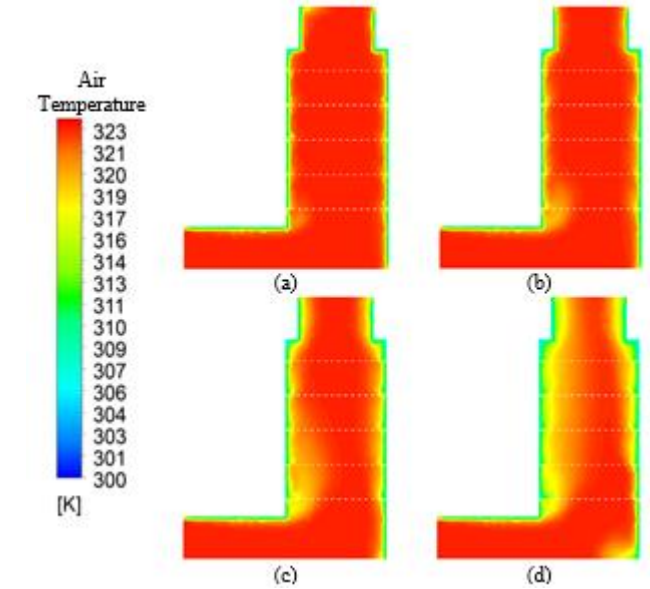

Fig. 5. Air temperature in middle plane (a) 4s, (b) 8s, (c) 16s, (d) 32s.

The air temperature distributions were plotted in the middle plane. It had a purpose to know different contours from time to time. It can be seen in Figure 5. At 4 seconds, the high air temperature was in the middle position and air near the wall had a low temperature. At 8 seconds, in the top corner, there was a small discoloration from red to yellow. The discoloration looked like yellow fog. It meant the top corner was an initial position for air temperature change. The discoloration grows up from time to time until 32 seconds.

It meant air temperature inside the cabinet underwent the mixing process. In this simulation, the wall temperature influenced the heating process. Based on Figure 5, the inlet air temperature mixed wall temperature. It was because the air touched the wall. It is called conduction heat transfer.

D. Air Temperature Distribution in Each Tray

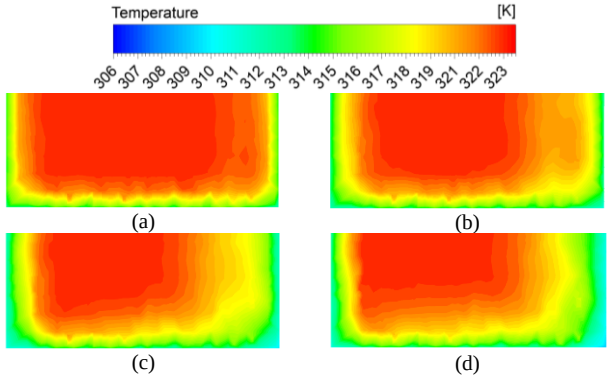

Fig. 6. Air temperature distribution in tray 1 (a) 4s, (b) 8s, (c) 16s, (d) 32s.

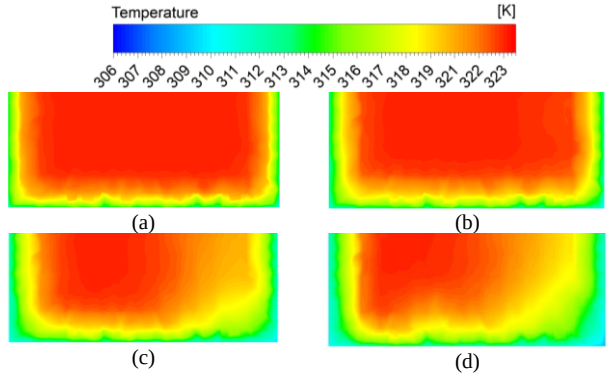

Fig. 7. Air temperature distribution in tray 2 (a) 4s, (b) 8s, (c) 16s, (d) 32s.

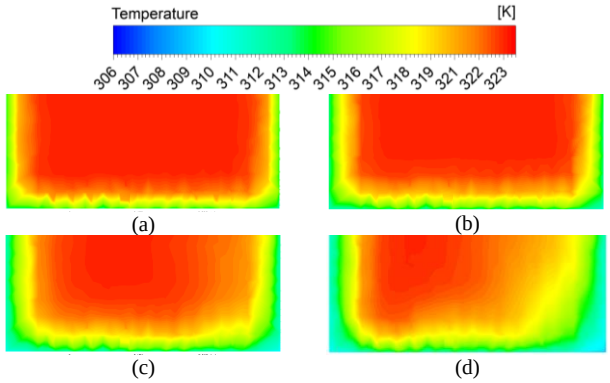

Fig. 8. Air temperature distribution in tray 3 (a) 4s, (b) 8s, (c) 16s, (d) 32s.

The air temperature in each tray was analyzed. There were tray positions and time change. It had a purpose to know the air temperature distribution from time to time and the optimal tray position. It showed in Figure 6 until Figure 10. The temperature contour was showed for half side of the tray for

each tray because the temperature contours of the other half side were the same.

It a showed hot air position was in the center for all of the trays. It was because trays had many holes in the surface. It caused hot air from the inlet section could through directly. Meanwhile, air temperatures were low in the corner edge of the tray. Based on Figure 6, the air temperature distribution was not uniform at 4 seconds. The air had high temperatures in the middle of the cabinet but the air near the wall still had low temperatures. At 8 seconds, the air temperature distribution was still not uniform. But the cold air temperature near the wall starts to mix with the hot air. It showed by discoloration inside the edge. At 16 seconds until 32 seconds, the air temperature distributions were more uniform than before. It meant the mixing process would happen if time was added. Based on Figure 6, the optimum tray position can be known. It was signed by red color. It showed hot air. The tray in the bottom position had more red color than other trays. It meant tray in the bottom position was optimal. It because the position was near to inlet hot air.

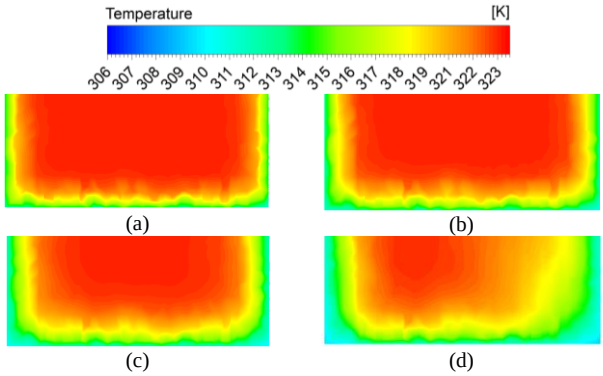

Fig. 9. Air temperature distribution in tray 4 (a) 4s, (b) 8s, (c) 16s, (d) 32s.

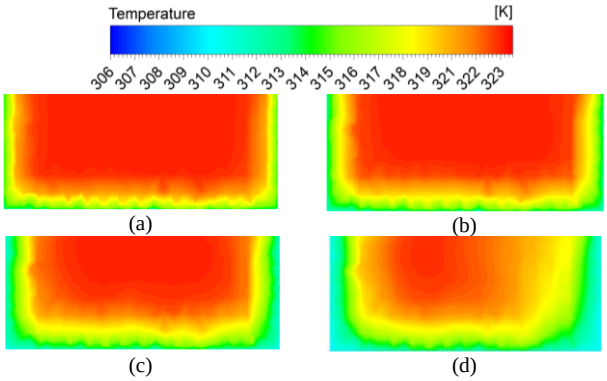

Fig.10. Air temperature distribution in tray 5 (a) 4s, (b) 8s, (c) 16s, (d) 32s.

E. Air Velocity Streamlinse in Each Tray

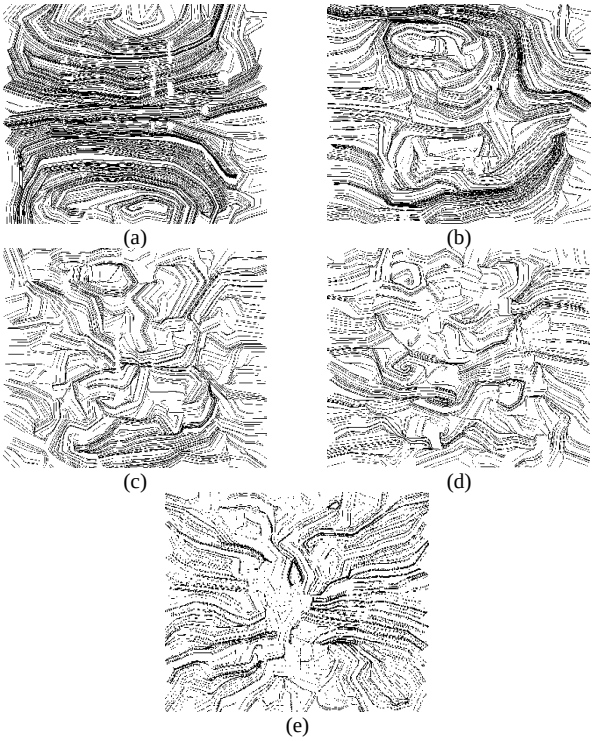

Fig.11. Air velocity streamlines in (a) tray 1, (b) tray 2, (c) tray 3, (d) tray 4, (e) tray 5.

Figure 11 shows air streamlines in each tray at 32 seconds. It had a purpose to ensure that the tray in the bottom position or tray 1 was optimum as explained in section air temperature distribution in each tray. Based on Figure 11 could be shown the different characteristics of airflow. It was shown by air velocity streamlines in each tray. Based on Figure 11a, air velocity streamlines in tray 1 showed two vorticities in the tray surface. The big vorticities in tray 1 showed that airflow rotation. It made the hot air mix with cold air so it could increase air temperature. Based on Figure 11, the optimum position in each tray could be predicted. It was signed by a vorticities position on the tray surface.

F. Air Velocity, Temperature, and Pressure in Centerline

.

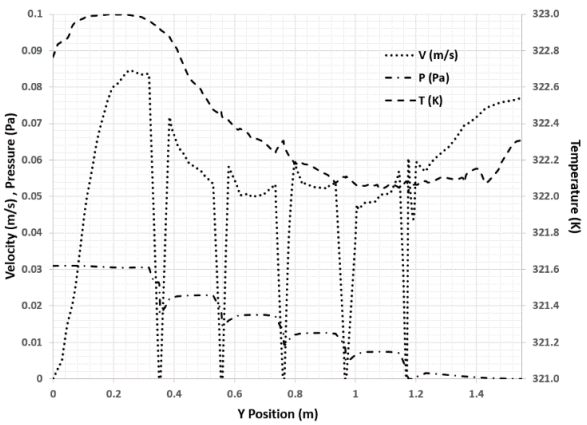

Fig.12. Air velocity, temperature, and pressure in centerline.

Figure 12 shows many parameters in the centreline at 32 seconds such as air velocity, temperature, and pressure. Based on Figure 12, air velocity decreased when air touched trays surface. It made backflows. The highest air velocity 0.084 m/s when the air in elbow position y = 0.3 m. The air velocity increased when the air went to the outlet section from y = 1.3 m to y = 1.55 m. It was 0.077 m/s.

The air temperature inside the drying cabinet decreased from y = 0 m to y = 1.55 m. It because of temperature conditions from trays and cabinet wall temperature. The air needs much time to heat the cabinet. The highest air temperature was 232 K in y = 0.2 until y = 0.3 m or in elbow position. Based on Figure, the optimum tray position could be known. In tray number one, the maximum air temperature was 322.6 K. It was tray number one because of the position near with inlet section. Based on the figure also could be known that tray number five had the lowest air temperature 322 K.

Based on Figure 12, the air pressure inside the drying cabinet decreases slowly from 0.03 Pa to 0. It was because of the open system for the drying cabinet. It meant air enters the cabinet and then went to the outside cabinet. When air touched trays the same with velocity, air pressure would be decreased.

V. Conclusion

The optimum tray position was tray 1. It was at the bottom of the drying cabinet. It because of the position near to the inlet section of hot air. It happens at 32 seconds. It was signed by the air temperature distribution was more uniform than other trays position. It was also proved by air velocity streamlines that form big vorticities in the tray surface. The air temperature distribution could be uniform if the number of iterations was increased.

Acknowledgment

The authors want to say thank you for Politeknik Elektronika Negeri Surabaya for event support and also for Power Plant Engineering Study Program.

References

[1] S. Hamdi, “Mengenal Lama Penyinaran Matahari Sebagai Salah Satu Parameter Klimatologi,” Ber. Dirgant., vol. 15, no. 1, pp. 7–16, 2014.

[2] A. Kumar and M.-H. Kim, “Thermal Hydraulic Performance in a Solar Air Heater Channel with Multi V-Type Perforated Baffles,” Energies, vol. 9, no. 7, p. 564, 2016.

[3] G. Grandi, A. Ienina, and M. Bardhi, “Effective Low-Cost Hybrid LED-Halogen Solar Simulator,” vol. 50, no. 5, pp. 3055–3064, 2014.

[4] S. Dogra, “Effect of artificial roughness on Thermal and Thermohydraulic efficiency in Rectangular Duct of a Double pass solar Air Heater by using transverse ribs on the absorber plate,” Int. J. Mod. Eng. Res., vol. 3, no. 4, pp. 2271–2274, 2013.

[5] T. K. Abdelkader, Q. Fan, E. S. Gaballah, S. Wang, and Y. Zhang, “Energy and exergy analysis of a flat-plate solar air heater artificially roughened and coated with a novel solar selective coating,” Energies, vol. 13, no. 4, 2020.

[6] S. K. Jain, R. Misra, A. Kumar, and G. Das Agrawal, “Thermal performance investigation of a solar air heater having discrete V-shaped perforated baffles,” Int. J. Ambient Energy, vol. 0, no. 0, pp. 1–9, 2019.

[7] E. A. Handoyo, D. Ichsani, Prabowo, and Sutardi, “Experimental studies on a solar air heater having v-corrugated absorber plate with obstacles bent vertically,” Appl. Mech. Mater., vol. 493, pp. 86–92, 2014.

[8] A. M. Aboghrara, B. T. H. T. Baharudin, M. A. Alghoul, N. M. Adam, A. A. Hairuddin, and H. A. Hasan, “Performance analysis of solar air heater with jet impingement on corrugated absorber plate,” Case Stud. Therm. Eng., vol. 10, pp. 111–120, 2017.

[9] A. Sanghi, R. P. K. Ambrose, and D. Maier, “CFD simulation of corn drying in a natural convection solar dryer,” Dry. Technol., vol. 36, no. 7, pp. 859–870, 2018.

[10] J. A. Duffie and W. A. Beckman, Solar engineering of thermal processes. Wiley, 2013.

[11] B. Jia, F. Liu, and D. Wang, “Experimental study on the performance of spiral solar air heater,” Sol. Energy, vol. 182, no. September 2018, pp. 16–21, 2019.